

# Dynamic consolidation of diamond powder into polycrystalline diamond

David K. Potter and Thomas J. Ahrens

Seismological Laboratory 252-21, California Institute of Technology, Pasadena, California 91125

(Received 26 February 1987; accepted for publication 2 June 1987)

The formation of a polycrystalline solid compact, by fusing an initially porous aggregate of diamond crystals under dynamic shock pressure (7.5–18 GPa), is shown to depend critically on the size of the initial crystals. Porous aggregates of 100–150  $\mu\text{m}$  diameter crystals upon shock compaction produced compacts. These exhibited pronounced fracturing of the individual crystals and showed no evidence of fusion. Aggregates consisting of ultrafine crystals ( $< 5 \mu\text{m}$ ) also exhibited minimal consolidation. However, samples composed of crystals in the range 4–8  $\mu\text{m}$  produced strong fused compacts of polycrystalline diamond. A model calculation indicates that at 10 GPa less than 0.07 mass fraction of the diamond powder can be melted and this molten material is quenched in 0.8 ns for 8- $\mu\text{m}$ -diam crystals.

We describe the conditions under which an initially porous aggregate of diamond single crystals fuses together to form a solid compact under moderate dynamic shock pressure (7.5–18 GPa). Formation of such a fused compact requires at least partial melting along the crystal boundaries and resolidification within the duration of the shocked state (otherwise the sample would disintegrate by tensile failure when rarefaction waves arrive at the compacted powder<sup>1</sup>). Figure 1 shows the proposed temperature and pressure range over which liquid carbon may exist.<sup>2–5</sup> Experimentally the high melting point of diamond is difficult to achieve. Gold *et al.*<sup>6</sup> melted a portion of the (100) face of a single-crystal diamond anvil (at  $> 12$  GPa) with radiation from a Q-switched YAG laser and, more recently, Weathers and Bassett<sup>7</sup> melted 1  $\mu\text{m}$  diamond particles at 30 GPa in a diamond anvil cell using a pulsed YAG laser. Venkatesan *et al.*,<sup>8</sup> Steinbeck *et al.*,<sup>9</sup> and Braunstein *et al.*<sup>2</sup> melted graphite with a pulsed ruby laser at pressures of less than 0.1 GPa, and all experiments indicated a melting temperature of about 4300 K. The latter study indicated that the liquid evaporates at about 4700 K.

In the present experiments we shocked initially porous samples of diamond single crystals to induce partial melting. We show that continuum temperature calculations (which imply that shock-induced deformation occurs uniformly) do not, for our experimental conditions, give sufficiently high temperatures, for melting to occur. We sought to establish whether shock compaction induces sufficiently high temperatures to produce melting on grain boundaries.

Previous studies suggest that frictional heating from crystal boundary sliding in diamond<sup>10,11</sup> or shear band deformation in ceramic materials,<sup>12</sup> could induce higher temperatures than predicted via continuum calculations. The present experiments were conducted on different sizes of natural and synthetic diamond crystals, since the strength of metal or ceramic compacts is often observed to increase with decreasing particle size according to a Hall-Petch relation.<sup>13,14</sup> Also, the model of Schwartz *et al.*<sup>15</sup> of shock-wave consolidation of metal powders predicts that, as the particle diameter  $d$  is reduced, the properties of the compact are preserved provided the characteristic times in the shock-consolidation process are scaled with  $d^2$ .

Shock compaction was performed using flyer plate impact and a momentum trapping recovery system (see inset, Fig. 1).<sup>16,17</sup> Stainless-steel flyer plates (16 mm in diameter and 2.5 mm thick) with velocities of 1.8 to 2.0 km/s were impacted against stainless-steel dish-shaped capsules (inner diameter 7 mm, thickness 3 mm) containing the diamond crystals. These induced shock pulses with  $\sim 0.8 \mu\text{s}$  durations. A 0.5-mm-thick disk (single crystal) of  $\text{Al}_2\text{O}_3$  was placed between the stainless steel and the diamond crystals so as to prevent metal interacting with the diamond.

Scanning electron microscopy (SEM) of the 100–150  $\mu\text{m}$  natural diamond crystals from shots 885 and 888 (Table I) revealed that the samples were compacted and their bulk density was very high ( $\sim 95$ –99% of the crystal density), as indicated by a lack of voids between grains, although a high

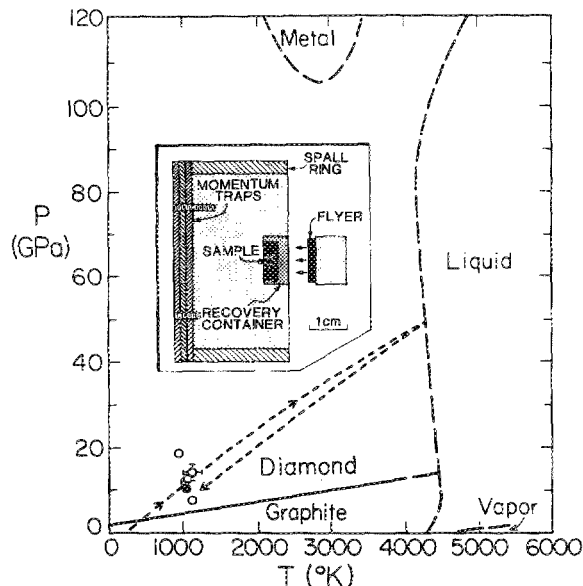


FIG. 1. Shock pressures and continuum temperatures (Table I) and proposed phase diagram of carbon.<sup>2–5</sup> Solid and open symbols indicate fused and unfused compact continuum shock temperatures. Proposed thermodynamic path at grain boundaries indicated by short dashed curve. Diamond-diamond impacts producing higher pressures and temperatures than continuum values. Inset shows sketch of experimental assembly.

TABLE I. Experimental conditions and calculated shock pressures and temperatures.

Shot number	Initial sample	Initial density (% of crystal density)	Projectile velocity (km/s)	Shock <sup>a</sup> pressure (GPa)	Shock temperature (K)	Recovered sample condition
885	100–150 μm natural diamond	68	1.90	18.2	920	compacted, no fusion
888	100–150 μm natural diamond	55	2.01 ± 0.20	14.1 ± 2.0	1140 ± 120	compacted, no fusion
891	4–8 μm synthetic diamond powder	50	1.81	10.8	1040	fused compact
901	< 5 μm synthetic diamond powder	55	1.81 <sup>b</sup>	12.0	1020	unconsolidated
904	< 5 μm synthetic diamond powder	38	1.81	7.5	1140	unconsolidated
907	4–8 μm synthetic diamond powder	50	1.81	10.8	1040	fused compact
910	100 μm synthetic diamond	55	1.86	12.7	1050	compacted, no fusion

<sup>a</sup> Initial shock state.

<sup>b</sup> Inferred from propellant mass.

degree of fracturing was observed in the individual crystals [Fig. 2(b)]. The 100-μm synthetic diamond crystals (shot 910) behaved similarly. There was no evidence of melting at crystal boundaries in the 100-μm natural and synthetic recovered samples. The tensile strength of the compacts was only moderate since it was possible to remove individual grains with a steel probe.

Samples from shots 901 and 904 (< 5 μm synthetic diamond crystals) were observed to be very unconsolidated. Much of the material was loose powder, while more “consolidated” regions were very friable. These latter regions consisted of clumps of individual particles with no evidence of fusion [Fig. 2(d)].

Recovered material formed from 4–8 μm synthetic diamond crystals (shots 891 and 907) revealed clear evidence of fusion between crystals, emphasized by the inability to distinguish original crystal boundaries in many regions of the SEM images [see region bounded by square in Fig. 2(f)]. Moreover, the tensile strength of the fused compacts was high as judged by the difficulty to remove crystals with the steel probe, and by the deposition of steel onto the sample surfaces when scored by the probe. Debye–Scherrer x-ray analyses of samples from all experiments demonstrated that no detectable graphite was formed.

Hugoniot for the porous diamond samples were constructed using the shock ( $U_s$ ) and particle ( $u_p$ ) velocity data of Pavlovskii for diamond ( $3.51 \text{ Mg/m}^3$ ),

$$U_s \text{ (km/s)} = 12.16 + 1.00u_p, \quad (1)$$

and Eq. (11.40) of Zeldovich and Raizer<sup>19</sup> and an assumed Grüneisen parameter  $\gamma$  of 0.9.<sup>18</sup> Shock pressures ( $P_H$ ) were

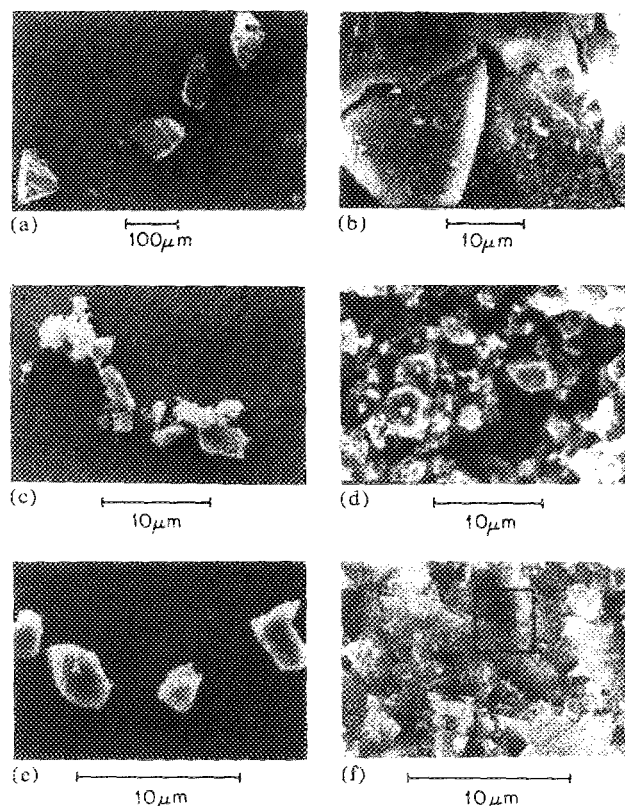


FIG. 2. SEM images illustrating: (a) 100–150 μm natural diamond crystals, unshocked. (b) Fractures produced in shocked 100–150 μm natural diamond crystals (shot #888). (c) < 5 μm synthetic diamond crystals, unshocked. (d) Unconsolidated sample from shocked < 5 μm synthetic diamond crystals (shot #901). (e) 4–8 μm synthetic diamond crystals, unshocked. (f) Fused compact formed from 4–8 μm synthetic diamond crystals (shot #891).

obtained using the impedance matching technique.<sup>19</sup> The shock (continuum) temperature  $T_H$  was calculated from<sup>19</sup>

$$T_H = T_s + \frac{V_H(P_H - P_s)}{\gamma C_v}, \quad (2)$$

where  $T_s$  and  $P_s$  are the temperature and pressure along the principal isentropes,  $V_H$  is the high-pressure specific volume, and  $C_v$  is the specific heat (see pp. 700–701, Ref. 19). Values of  $P_H$  and  $T_H$  are given in Table I and shown in Fig. 1. The continuum temperatures were lower than those predicted for melting, implying that grain sliding friction induced sufficiently high temperatures at grain boundaries, to cause localized melting, and fuse the powder compacts.

The upper bound for the mass fraction,  $L$ , of melted material in a typical compacted diamond sample,  $\sim 0.07$ , may be estimated by assuming all the internal energy of the shock goes into melting material on the surface.<sup>15,16</sup>

$$L = \frac{P_H [(V_{00}/V_0) - 1] V_0}{2 [C_p (T_m - T_0) + H_m]}, \quad (3)$$

where  $P_H$  is taken as 10 GPa and  $V_0$  and  $V_{00}$  are the initial crystal and porous specific volumes, respectively. Here  $V_{00}/V_0 \approx 1.85$ . Also  $C_p$  is the specific heat at constant pressure, taken<sup>20</sup> to be 2 kJ/kg °C,  $(T_m - T_0)$  is the difference between melting and initial temperature, taken as 4000 K, and the heat of fusion,  $H_m$ , is 9.2 MJ/kg.<sup>5</sup> We assume that all of the melt is produced as a result of grain friction and coats the individual diamond single crystals.

In order to consolidate the sample material the duration time  $t_d$  of the shock pulse, 0.8  $\mu$ s, must exceed the time  $t_f$  it takes to conduct the excess heat in the molten carbon layer into the cooler interior of the diamond to freeze the diamond. In addition, one might also have to wait an additional time  $t_c$  to cool the hot diamond down to a temperature where it can withstand a moderate amount of tensile stress associated with unloading. Thus  $t_f$  is given by<sup>15</sup>

$$t_f = \frac{\pi D}{16} \left( \frac{L d H_m}{D C_p (T_m - T_0)} \right)^2, \quad (4)$$

where  $D$  is the mean thermal diffusivity of the diamond<sup>21</sup> ( $1 \times 10^{-4}$  m<sup>2</sup>/s) and  $d$  is the crystal diameter. For  $d = 8 \mu$ m a freezing time of 0.8 ns is obtained. We note that for the present experiments  $t_d$  easily exceeds this value. If we assume  $t_c = 0$  and put  $t_d = t_f = 0.8 \mu$ s we obtain a critical size for  $d \sim 250 \mu$ m, above which fracturing and not consolidation may occur. Experimentally we observe fracturing in 100–150  $\mu$ m crystals in agreement with this prediction.

For very small crystals the time constant for thermal equilibrium between the surface and interior  $t_e$  ( $\approx d^2/D$ ) ap-

proaches the shock transit time  $t_s$  ( $= d/U_s$ ) through the crystal. Notably,  $t_s$  becomes only comparable with  $t_e$  at  $d = 0.1 \mu$ m. Here  $t_s = 0.02$  ns and  $t_e = 0.1$  ns. Thus surface melting and fusion, and hence consolidation, are predicted not to take place in ultrafine crystals. Lack of surface fusion is already evident upon compaction of  $< 5 \mu$ m powder, which only qualitatively agrees with this prediction.

This work was supported by the National Science Foundation and under the C.I.T. Program for Advanced Technologies (sponsored by GTE, TRW, Aerojet General, and General Motors) contribution number 4443, Division of Geological and Planetary Sciences. We appreciate the help of Dr. John Armstrong, Dr. Ian Hutcheon, and Cheryl Brigham in obtaining the SEM images, and Dr. Liselotte Schioler and an anonymous reviewer for helpful comments on the manuscript.

<sup>1</sup>W. H. Gourdin, *Prog. Mater. Sci.* **30**, 39 (1986).

<sup>2</sup>G. Braunstein, J. Steinbeck, M. S. Dresselhaus, G. Dresselhaus, B. S. Elman, T. Venkatesan, B. Wilkens, and D. C. Jacobsen, *Beam Solid Interactions and Phase Transformations: Proceedings of the Materials Research Society (Boston)*, edited by H. Kurz, G. L. Olson, and J. M. Poate, **51**, 233 (1986).

<sup>3</sup>F. P. Bundy, *J. Geophys. Res.* **85**, 6930 (1980).

<sup>4</sup>J. W. Shaner, J. M. Brown, C. A. Swenson, and R. G. McQueen, *J. Phys. (Paris)* **45**, C8-235 (1984).

<sup>5</sup>J. A. Van Vechten, *Phys. Rev. B* **7**, 1479 (1973).

<sup>6</sup>J. S. Gold, W. A. Bassett, M. S. Weathers, and J. M. Bird, *Science* **225**, 921 (1984).

<sup>7</sup>M. S. Weathers and W. A. Bassett, *Phys. Chem. Min.* (to be published).

<sup>8</sup>T. Venkatesan, D. C. Jacobsen, J. M. Gibson, B. S. Elman, G. Braunstein, M. S. Dresselhaus, and G. Dresselhaus, *Phys. Rev. Lett.* **53**, 360 (1984).

<sup>9</sup>J. Steinbeck, G. Braunstein, M. S. Dresselhaus, T. Venkatesan, and D. C. Jacobsen, *J. Appl. Phys.* **58**, 4374 (1985).

<sup>10</sup>F. P. Bowden and A. E. Hanwell, *Nature* **201**, 1279 (1964).

<sup>11</sup>F. P. Bowden, C. A. Brookes, and A. E. Hanwell, *Nature* **203**, 27 (1964).

<sup>12</sup>D. R. Schmitt and T. J. Ahrens, *Geophys. Res. Lett.* **10**, 1077 (1983).

<sup>13</sup>E. O. Hall, *Proc. Phys. Soc. B* **64**, 747 (1951).

<sup>14</sup>N. J. Petch, *J. Iron and Steel Institute* **174**, 25 (1953).

<sup>15</sup>R. B. Schwarz, P. Kasiraj, T. Vreeland, Jr., and T. J. Ahrens, *Acta Metall.* **32**, 1243 (1984).

<sup>16</sup>T. J. Ahrens, D. Kostka, P. Kasiraj, T. Vreeland, Jr., A. W. Hare, F. D. Lemkey, and E. R. Thompson, *Rapid Solidification Processing of Principles and Technologies III*, edited by R. Mehrabian (National Bureau of Standards, 1983), p. 672.

<sup>17</sup>J. Vizgirda, T. J. Ahrens, and F.-D. Tsay, *Geochim. Cosmochim. Acta* **22**, 1059 (1980).

<sup>18</sup>M. N. Pavlovskii, *Sov. Phys. Solid State* **13**, 741 (1971).

<sup>19</sup>Y. Zeldovich and Y. P. Raizer, *Physics of Shock Waves and High Temperature Hydrodynamic Phenomena*, Vol. 2 (Academic, New York, 1967).

<sup>20</sup>R. A. Robie, B. S. Hemingway, and J. R. Fisher, *U. S. Geol. Survey Bull.* No. 1452, 1978.

<sup>21</sup>S. P. Clark, Jr., in *Handbook of Physical Constants*, edited by S. P. Clark, Jr., *Geol. Soc. Am. Mem.* **97**, 459 (1966).